Enhancing Selective Ammonium Transport in Membrane Electrochemical Systems

Kai Yang, Mohan Qin*

Department of Civil and Environmental Engineering, University of Wisconsin–Madison, Madison, WI 53706, United States

* Corresponding author. E-mail: mohan.qin@wisc.edu; Tel: +1 (608) 265-9733

ABSTRACT

Recovering ammonia nitrogen from wastewater is a sustainable strategy that simultaneously addresses both nitrogen removal and fertilizer production. Membrane electrochemical system (MES), which utilizes electrochemical redox reactions to transport ammonium ions through cation exchange membranes, has been considered as an effective technology for ammonia recovery from wastewater. In this study, we develop a mathematical model to systematically investigate the impact of co-existing ions on the transport of ammonium (NH_4^+) ions in MES. Our analysis elucidates the importance of pH values on both the NH_4^+ transport and inert ion (Na^+) transport. We further comprehensively assess the system performance by varying the concentration of Na^+ in the system. We find that while the inert cation in the initial anode compartment competes with NH_4^+ transport, NH_4^+ dominates the cation transport in most cases. The transport number of Na^+ surpasses NH_4^+ only if the fraction of Na^+ to total cation is extremely high (>88.5%). Importantly, introducing Na^+ ions into the cathode compartment significantly enhances the ammonia transport due to the Donnan dialysis. The analysis of selective ion transport provides valuable insights into optimizing both selectivity and efficiency in ammonia recovery from wastewater.

KEYWORDS

Selective ammonia recovery, membrane electrochemical system, ion transport, Donnan dialysis, transport number, selectivity.

19

20

21 **TOC ART**

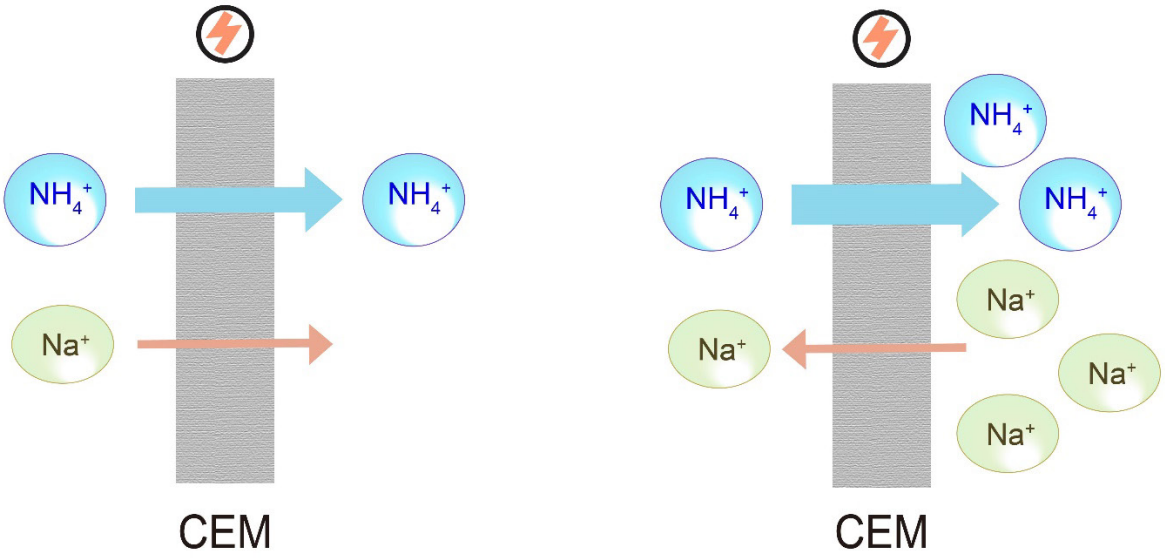

22

23

1. INTRODUCTION

The production of nitrogen fertilizer enabled by the Haber-Bosch process has boosted the rapid growth of the world population since a century ago, with half of the nitrogen atoms in humans today originating from it (Chen et al., 2018; Dawson and Hilton, 2011). While this process is considered the most impactful invention of the 20th century, it consumes more than 1% of global energy and accounts for 1.6% of global greenhouse gas emissions (Capdevila-Cortada, 2019; Ertl, 1990; Jacobsen et al., 2001). About 30% of the ammonia (NH_3) produced from the Haber-Bosch process ends up in wastewater, mainly in the form of ammonium ions (NH_4^+) (Galloway et al., 2004a). An excess amount of ammonium ions in wastewater might contaminate the environment and therefore requires further treatment in wastewater treatment plants (WWTPs) to satisfy the discharge requirements (Galloway et al., 2004b; Van der Hoek et al., 2018). Instead of consuming energy to convert ammonium ions back to nitrogen gas using the nitrification-denitrification process in WWTPs, direct recovery is considered a more sustainable approach to simultaneously remove ammonia from wastewater and utilize ammonia for fertilizer production (Burns and Qin, 2023; Yang et al., 2023; Zamora et al., 2017).

In recent years, electrochemical approaches, such as bioelectrochemcial system (BES), electrochemical stripping (ECS), electrosorption, and electrodialysis (ED), have been demonstrated to effectively recover ammonia from various types of wastewater by utilizing current

to transport ammonium ions (Fang et al., 2018; Kuntke et al., 2017; Lee et al., 2020; Qin and He, 2014; Qin et al., 2016; Tarpeh et al., 2018; Yang and Qin, 2021; Ye et al., 2019; Zou et al., 2017). Among these processes, both BES and ECS are electro-driven processes, with the catalyst for BES anode being microorganisms and the reaction in ECS anode being abiotic (Rodríguez Arredondo et al., 2015). Here, they are collectively referred to as membrane electrochemical systems (MES) to represent the technology platform that relies on redox reactions for current generation and ammonia recovery. MES utilizes the electron transfer to transport NH_4^+ across cation exchange membranes (CEMs) to the cathode for charge balance. In MES, the pH gradient created by the electrochemically generated H^+ and OH^- at the anode and the cathode, respectively, establishes a concentration gradient for NH_4^+ across the CEM which facilitates the transport of ammonium ions (Liu et al., 2016). The ammonia in the catholyte can be recovered by stripping, acid adsorption, forward osmosis, and transmembrane chemisorption and the produced fertilizer can be used to improve crop growth (Kuntke et al., 2012; Ledezma et al., 2015; Liu et al., 2020; Rodrigues et al., 2022a; Rodrigues et al., 2020; Rodríguez Arredondo et al., 2015; Tarpeh et al., 2018; Zhang and Angelidaki, 2015a).

Cation exchange membrane (CEM) plays a critical role in MES for ammonia recovery. In the CEM, the fixed negatively charged groups (e.g., sulfonate groups) within the crosslinked polymer matrix enable cation permeation and inhibit anion transport (Luo et al., 2018; Strathmann, 2010).

59 NH_4^+ ion, which has a relatively small hydrated ionic size (0.331 nm) and fast diffusivity in CEM,
60 can be easily transported across the membrane and serve as excellent charge carriers in BES and
61 regular electrochemical system (Epsztein et al., 2019; Liu et al., 2016). Since NH_4^+ is not used as
62 a substrate in the redox reactions, its transport in MES is a physicochemical process (Kim et al.,
63 2008). Therefore, MES shares the same mechanisms (i.e., diffusion and migration) for the transport
64 of NH_4^+ and other cations.

65 To improve the performance of MES for ammonia recovery, researchers have focused on the
66 improvement of reactor configuration and adjustment of operation parameters (e.g., loading ratio,
67 current density, etc.), aiming at improved ammonia recovery rate and efficiency as well as reduced
68 energy consumption (Cord-Ruwisch et al., 2011; Kuntke et al., 2012; Lee et al., 2020; Zhang and
69 Angelidaki, 2015b; Zou et al., 2017). However, the selectivity of NH_4^+ ions compared to other
70 cations across the CEM, which distinguishes the transport of NH_4^+ ions from other cations, has not
71 yet been systematically evaluated. In the MES for ammonia recovery, the anode is fed with
72 wastewater, in which other cations, such as Na^+, K^+, and Ca^{2+}, are ubiquitous besides NH_4^+ ions,
73 with Na^+ ion being the most dominant competing cation species (Park et al., 2006; Tarpeh et al.,
74 2018). While the transport of these cations does not directly interact with the transport of NH_4^+
75 ions, it is also driven by the potential gradient and would potentially impact the ammonium
76 transport. In addition, the competing cations in the cathode compartment could lead to Donnan

77 Dialysis, a concentration-gradient driven process for ion exchange across the CEM, which may
78 theoretically facilitate the transport of ammonium ions (Chen et al., 2020; Chen et al., 2021; Davis,
79 2000b).

80 In this study, we developed a dynamic mathematical model to systematically investigate the ion
81 transport behaviors in MES. Specifically, we analyzed the pH variation along with the NH_4^+
82 concentration profile and the inert ion (Na^+) concentration profile in MES. We further adjusted the
83 concentration of Na^+ in the system and evaluated its effect on both transmembrane transport of
84 ions and ammonia recovery performance. The impact of anolyte Na^+ concentration, anolyte Na^+
85 fraction, and catholyte Na^+ concentration was investigated. Moreover, the selectivity of NH_4^+ to
86 the inert ion (Na^+) was also studied to characterize the selective ammonia recovery by the
87 electrochemical system.

2. MES PROCESS MODEL

2.1. MES Process and Operation

88
89 The model performed in this study is based on a 24 h batch experiment in an membrane
90 electrochemical system (MES) reactor (Figure 1). The reactor is composed of two compartments,
91 an anode compartment and a cathode compartment, divided by a cation exchange membrane. Two
92 electrodes, one carbon brush electrode and one carbon cloth electrode, are installed in anode and
93 cathode compartments, respectively, connected by an external resistor. The anode and cathode

compartments are initially filled with synthetic wastewater and deionized water, respectively. A detailed recipe for synthetic wastewater is listed in Table S1. In the anode, acetate is oxidized by exoelectrogens with electrons being captured in the anode electrode and transferred to the external circuit. At the cathode, oxygen serves as the electron acceptor. The NH_4^+ in the anolytes moves towards the catholyte, driven by both the potential gradient and concentration gradient. The high pH at catholytes converts NH_4^+ into NH_3, which can be stripped out of the cathode compartment by aeration and recovered using acid adsorption.

2.2. Mathematical Model for MES

An MES model is employed to describe the electrochemical reactions and transport of various species across the CEM in MES. Several assumptions are made to simplify the model. We assume that the acid-base reactions are infinitely fast so that the acid-base equilibria can be directly used in ionic mass balance. The CEM is considered as an ideal membrane with negligible water transport across the membrane and the charge density remains constant. Besides, the reactor compartment is assumed to be well mixed. The temperature is constant spatially and temporally. The specific values used for membrane properties and reactor geometry are summarized in Table S2. In the model, the transport of Na^+, NH_4^+, H^+, Ac^- (acetate ion), Cl^-, HCO_3^-, CO_3^{2-}, OH^-, NH_3, H_2CO_3, and HAc is considered. Their chemical reactions and the redox reactions at electrodes are modeled as generation/consumption terms in mass balances. The gas-solution equilibria for both

112 CO_2 and NH_3 are present by applying Henry's Law to derive the gas flux. The equilibrium
113 constants and Henry's Law constants are listed in Table S3.

114 This model has been developed and validated in our previous studies (Liu et al., 2016). It relies
115 on the Poisson-Nernst-Planck equation for describing ion transport in both the electrolyte and
116 CEM, while Donnan equilibrium is enforced at the CEM-anolyte/catholyte interface. The
117 boundary layer thickness is fixed at 0.2 mm in this model. In a recent study, the boundary layer is
118 associated with the current and affects the ion transport selectivity (Rodrigues et al., 2022b). The
119 key governing equations and all the acid-base reactions used in the model are described in
120 the Supplementary Information.

121 *2.3 Key Performance Parameters*

122 To characterize the performance of ammonia recovery, we investigate the selectivity of NH_4^+
123 over Na^+, which is defined as (He et al., 2018):

$$\rho\left(\frac{NH_4^+}{Na^+}\right) = \frac{\Delta c_{NH_4^+}/c_{NH_4^+,0}}{\Delta c_{Na^+}/c_{Na^+,0}} \quad (1)$$

124 where $\rho\left(\frac{NH_4^+}{Na^+}\right)$ is the selectivity of NH_4^+ over Na^+, $\Delta c_{NH_4^+}$ and Δc_{Na^+} are the concentration loss of
125 NH_4^+ and Na^+ at anode compartment, respectively, $c_{NH_4^+,0}$ and $c_{Na^+,0}$ are the initial concentration
126 of NH_4^+ and Na^+ in the anode compartment, respectively. The concentration losses of NH_4^+ and
127 Na^+ are defined as:

$$\Delta c_{NH_4^+} = c_{NH_4^+,t} - c_{NH_4^+,0} \quad (2)$$

$$\Delta c_{Na^+} = c_{Na^+,t} - c_{Na^+,0} \quad (3)$$

where $c_{NH_4^+,t}$ and $c_{Na^+,t}$ are the concentration of NH_4^+ and Na^+ at time of t in the anode compartment, respectively.

The transport number of ionic species i is denoted as t_i, the ratio of charge flux carried by ion i to the total charge flux of all ions, which equals to the charge carried by the electrons through the external circuit. The calculation of transport number t_i is described as:

$$t_i = \frac{z_i J_i}{\sum z_i J_i} = VFz_i \frac{c_{i,0} - c_{i,t}}{\int_0^t I_{tot}\, dt} \quad (4)$$

where z_i and J_i are the charges and the flux of the species i, respectively, and $c_{i,0}$ and $c_{i,t}$ are the concentrations of species i at the time of 0 and t, respectively, V is the volume of the compartment, F is the Faraday constant, I_{tot} is the current in the external wire, and $\int_0^t I_{tot}\, dt$ is the total charge transferred through the external wire from time 0 to t.

The ammonia recovery amount Q_{NH_3} is the total ammonia nitrogen concentration change, and the ammonia recovery efficiency η_{NH_3} is the ratio of ammonia recovery amount to the initial total ammonia nitrogen concentration.

$$Q_{NH_3} = c_{NH_4^+,0} + c_{NH_3,0} - c_{NH_4^+,t} - c_{NH_3,t} \quad (5)$$

$$\eta_{NH_3} = \frac{Q_{NH_3}}{c_{NH_4^+,0} + c_{NH_3,0}} \quad (6)$$

where $c_{NH_3,0}$ and $c_{NH_3,t}$ are the concentration of ammonia concentration at time of 0 and t.

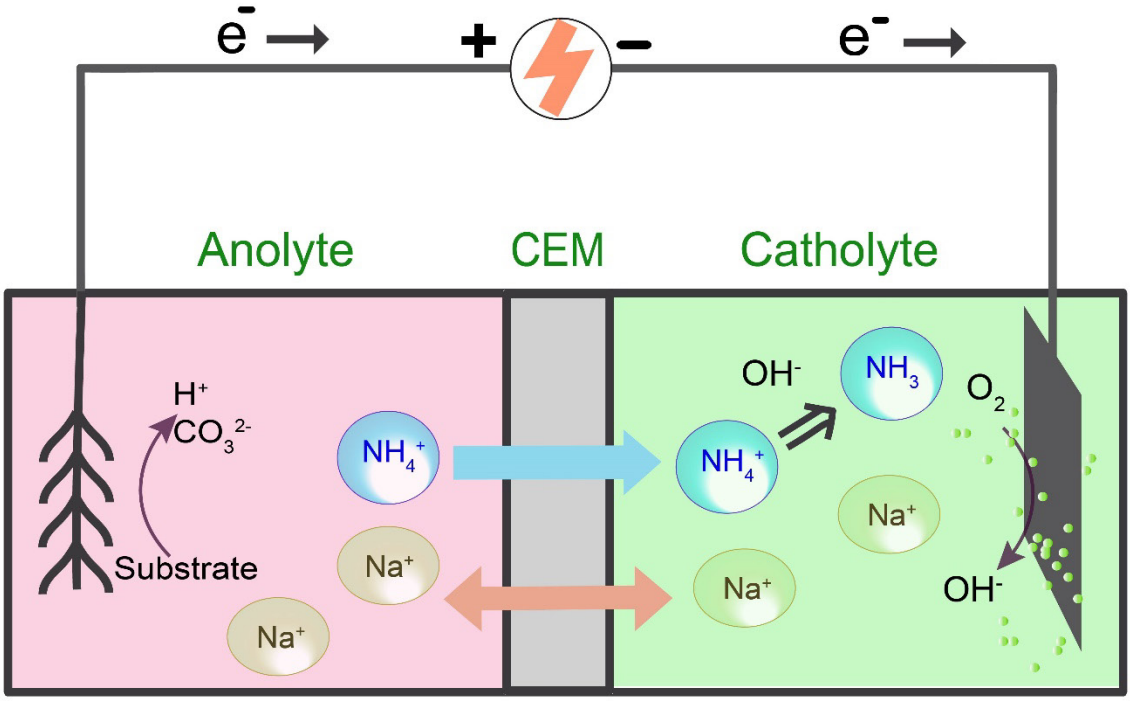

141

142 **Figure 1.** Schematic of the membrane electrochemical system (MES) for ammonia recovery.

3. RESULTS AND DISCUSSION

143 *3.1 Ion Concentration and pH Profiles*

144 To understand the transport behavior of various ions including Na^+, acetate (Ac^-), NH_4^+, HCO_3^-,

145 and CO_3^{2-}, the spatial and temporal concentration of these ions is investigated, based on a 24-hour

146 batch cycle with the current density linearly decreasing from 2 to 0.5 A m^{-2} in MES. The initial

147 concentrations of Na^+ and NH_4^+ ions in the anode compartment are 45 and 55 mmol·L^{-1},

148 respectively, to simulate the anaerobic digestate of livestock waste, while the cathode compartment
149 is filled with deionized water (Liu et al., 2016).

150 The normalized ion concentrations in the anode compartment are shown as a function of time
151 in Fig. 2A, and the pH profiles in anolyte and catholyte are illustrated in Fig. 2B. For all cations,
152 the concentration gradually decreased during the 24-hour batch cycle as a result of movement
153 towards the cathode compartment, which is caused by electrical force and concentration gradient.
154 Although the electrical potential gradient is identical for both monovalent cations, the differences
155 in concentration and variations in diffusion coefficient result in distinct effects on their transport
156 behaviors. Compared to Na^+ ions which serve as the competing ions, more NH_4^+ ions are
157 transported across the membrane. At the end of the simulation, Na^+ normalized concentration
158 reaches the value of 0.93, while NH_4^+ reaches 0.65. NH_4^+ ion has a larger initial concentration and
159 diffusion coefficient compared to Na^+, thus its concentration variation with time is also more than
160 that of Na^+. Additionally, normalized anode Ac^- concentration reached a value of 0.70, which can
161 be attributed to the oxidation by the microbial community. The consumption of acetate ions leads
162 to the formation of carbonic acid in the anode, creating an acidic environment in the anode and
163 shifting the NH_4^+/NH_3 equilibrium. As shown in Fig. 2B, the anolyte undergoes continuously
164 acidification, with its pH value decreasing from 7.61 to 5.92 during one batch cycle. Moreover,
165 the excess H^+ in the acidic environment would convert CO_3^{2-} and HCO_3^- into H_2CO_3, decreasing

166 their concentrations in the anode compartment. In the catholyte, the pH value increases rapidly at
167 the beginning of the batch, reaching a maximum value of 10.43 at 2.3 hour, and then steadily
168 decreases to 9.61 at the end of the batch cycle.

169 To comprehensively investigate the transport of cations across the cation exchange membrane
170 (CEM), the pH profiles (Fig. 2C), NH_4^+ concentration profiles (Fig. 2E), and Na^+ concentration
171 profiles (Fig. 2D) at three reaction times are demonstrated. The reaction times of 0.1, 10, and 20
172 hours are selected to represent the starting stage, the middle stage, and the final stage of the
173 simulation, respectively. The whole reactor is divided into three parts, anolyte, CEM, and catholyte,
174 with two membrane solution interfaces (MSI). At the MSI, the pH and ion concentrations are
175 different at each side of the interface due to the Donnan equilibrium.

176 The pH inside the CEM is always lower than that in the solutions while NH_4^+ and Na^+
177 concentrations are higher in solutions than in the CEM. This is attributed to the presence of fixed
178 negatively charged sulfonate groups within the crosslinked polymer chains of CEM, which results
179 in a significantly lower number of mobile anions in CEM than that of cations. The pH is critical in
180 ammonia recovery as it influences the equilibrium between NH_3 and NH_4^+. The pH at the anode
181 consistently decreases. For example, the pH values in the anolyte are 7.58, 6.41, and 6.02 at 0.1 h,
182 10 h, and 20 h, respectively. However, the pH at the cathode initially increases and then decreases.
183 The highest pH value in the catholyte is 10.43 after 2.31 hours. The pH values in the catholyte are

9.71, 10.06, and 9.69 at 0.1 h, 10 h, and 20 h, respectively. The pH variation in the catholyte is affected by the current density. Initially, a high current density leads to the rapid oxygen reduction reaction, generating a large number of OH^- ions and leading to a high pH level. At this stage, the transport of NH_4^+ is slow and the conversion from NH_3 to NH_4^+ is insufficient to lower the pH at catholyte.As the current decreases, the production of OH- ions is slower than the formation of NH_3 molecule which consumes OH- ions, causing a slight pH decrease. The distinct pH changes in the anolyte and catholyte lead to different trend in the pH profile across the membrane. At 0.1 h, the pH value inside the membrane showed a decrease from 5.88 at the anolyte MSI to 5.27 at the catholyte MSI. However, at 10 h and 20 h, the trends are reversed. For example, at 20 h, the pH value increased from 4.23 at the anolyte MSI to 6.69 at the catholyte MSI.

The NH_4^+ and Na^+ concentrations at the anode decrease as a function of time. It can be observed that more NH_4^+ ions are transported across the CEM than Na^+ ions. For example, the NH_4^+ concentration in the anolyte decreases from 54.8 mM at 0.1 h to 37.3 mM at 20 h (Fig. 2E). In contrast, the Na^+ concentration varies slightly, changing from 45.1 mM at 0.1 h to 42.3 mM at 20 h (Fig. 2D). The increase of NH_4^+ concentration in the catholyte is significantly less than the decrease of NH_4^+ concentration in the anolyte. For example, the NH_4^+ concentration in the catholyte increases from 0.03 mM at 0.1 h to 2.37 mM at 20 h (Fig. 2E). This is because a portion of NH_4^+ ions are converted to NH_3 in the cathode compartment. We note that the Na^+ concentration

202 only shows a slight variation, changing from 0.16 mM at 0.1 h to 3.31 mM at 20 h (Fig. 2D). Inside
203 the membrane, the NH_4^+ concentration only exhibits minor variation across the membrane. For
204 example, at 10 h, the NH_4^+ concentrations are 2.48 mM and 2.45 mM at anolyte MSI and catholyte
205 MSI, respectively. We note that NH_4^+ concentration inside the membrane decreases along the
206 operating time, which is attributed to the equilibrium with the decreasing NH_4^+ concentration in
207 the anolyte. The NH_4^+ concentrations are 2.73 mM, 2.48 mM, and 2.32 mM at 0.1 h, 10 h, and 20h,
208 respectively, in the membrane at the anolyte MSI. Given that the charge density of functional group
209 in the membrane is fixed, Na^+ concentration inside the membrane increases as a function of time.
210 At the anolyte MSI, the Na^+ concentrations increase from 2.27 mM at 0.1 h to 2.68 mM at 20 h.
211 The selectivity of NH_4^+/Na^+ across the membrane-solution interface changes with time (Fig.
212 2F). At the early stage of the batch cycle, the selectivity increases from 0.52 at 0.1 h to the
213 maximum value of 6.72 at 5.67 h, followed by a decrease to a plateau of ~ 5.0 until the end of the
214 batch. The rapid selectivity increase at the early stage is attributed to the fast ammonium transport
215 driven by the high current density and concentration gradient. At the later stage of the batch cycle,
216 the decrease in current generation leads to a relatively stable transport ratio between NH_4^+ and Na^+.

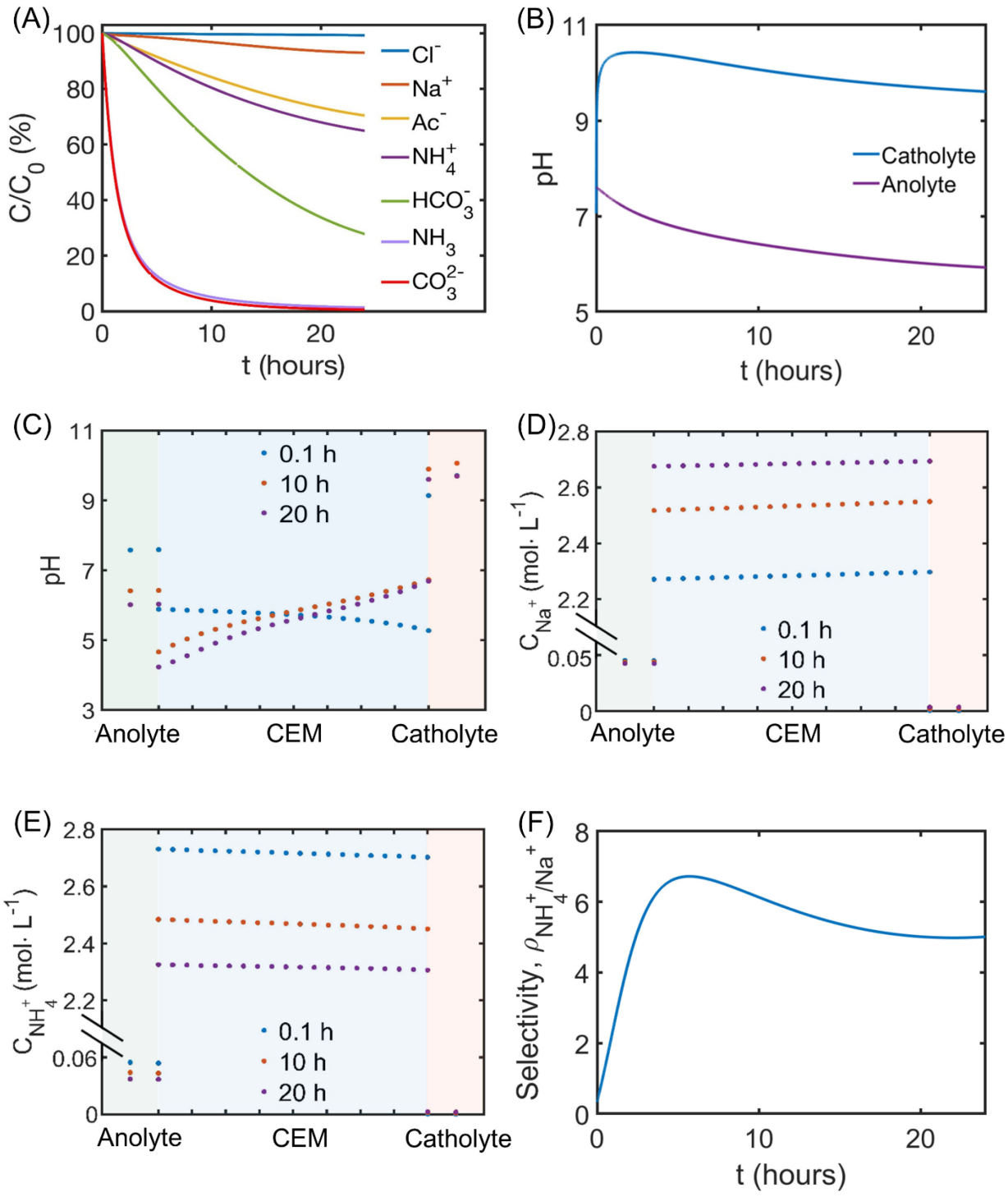
(A)
C/C0 (%)
t (hours)
Cl-
Na+
Ac-
NH4+
HCO3-
NH3
CO32-
(B)
pH
t (hours)
Catholyte
Anolyte
(C)
pH
0.1 h
10 h
20 h
Anolyte
CEM
Catholyte
(D)
CNa+ (mol· L-1)
0.1 h
10 h
20 h
Anolyte
CEM
Catholyte
(E)
CNH4+ (mol· L-1)
0.1 h
10 h
20 h
Anolyte
CEM
Catholyte
(F)
Selectivity, ρNH4+/Na+
t (hours)

217

Figure 2. Concentration and pH profiles in the membrane electrochemical system. Current linearly decreases from 2.0 to 0.5 A m^{-2} during a 24-hour batch cycle. The wastewater fed into the anode compartment contains 55 mmol·L^{-1} ammonium ions (NH_4^+) and 45 mmol·L^{-1} sodium ions (Na^+), whereas the cathode compartment is filled with deionized water. (A) Normalized ion concentration C/C_0 of the major ions in the anode compartment as a function of time. C is the ion concentration in the anode at time t, and C_0 is the initial ion concentration. (B) Anolyte and catholyte pH values as a function of time. (C) pH profile at 0.1 h, 10 h, and 20 h. (D) Na^+ concentration at 0.1 h, 10 h, and 20 h. (E) NH_4^+ concentration at 0.1 h, 10 h, and 20 h. For C, D, and E, green zones at the left represent anolyte, and the orange zones at the right represent catholyte, with CEM membrane in the middle (blue zones). (F) The selectivity of NH_4^+/ Na^+ across the membrane-solution interface changes with time. At the membrane-solution interface, the pH and concentrations of cations are different at each side of the interface because of the Donnan equilibrium.

3.2 Effect of Na^+ concentration in the anode

Wastewater may contain multiple kinds of ions with varying concentrations, making the selective transport of NH_4^+ critical. The impact of the inert cation concentrations on the ammonium transport is investigated by evaluating the key system metrics such as removal efficiencies, transport numbers, selectivity, and ammonia recovery amounts and efficiencies for both Na^+ and

236 NH_4^+ ions. Here, we change the initial anode Na^+ concentration from 1 mmol·L^{-1} to 200 mmol·L^{-1} while the initial concentration of NH_4^+ in the anode compartment is maintained at 55 mmol·L^{-1}.

238 As shown in Fig. 3A, the concentration of NH_4^+ expressed as normalized concentration is consistently lower than that of Na^+, indicating a higher transfer efficiency of NH_4^+ ions per unit of initial concentration than Na^+ ions regardless of the concentration of Na^+ in the anode compartment. Specifically, the normalized Na^+ concentration is constantly above 90.8% while the normalized NH_4^+ concentration is below 69.1%. This phenomenon can be attributed to the fact that NH_4^+ ions are more favorable to be transferred across CEM than Na^+ ions as illustrated in Section 3.1, and such preference is independent of the Na^+ concentration changes in the anolyte.

245 To compare the ion transfer efficiency, the transport numbers of both NH_4^+ and Na^+ ions are calculated and illustrated in Fig. 3B. The transport number is defined as the fraction of the total electric current carried by a particular ionic species transported across the membrane. As shown in Fig. 3B, the transport number of NH_4^+ is always higher than that of Na^+, indicating that the transport of NH_4^+ dominates the charge transfer. The transport number of NH_4^+ is close to unity and the Na^+ transport is minimal with the anode Na^+ concentration below 8 mmol·L^{-1}. However, as the anode Na^+ concentration increases from 8 mmol·L^{-1} to 120 mmol·L^{-1}, the transport number of NH_4^+ decreases from 0.95 to 0.79 while the transport number of Na^+ increases from 0.03 to 0.27. The decrease in the transport number of NH_4^+ confirms the presence of ion competition between

254 NH_4^+ and Na^+. To better characterize the ion competition, we calculated the selectivity of NH_4^+/
255 Na^+ in Fig. 3C. The lowest NH_4^+/ Na^+ selectivity is 4.2 when the anode Na^+ concentration is 8
256 mmol·L^{-1}. When the anode Na^+ concentration decreases from 8 mmol·L^{-1} to 1 mmol·L^{-1}, the
257 selectivity constantly increases from 4.2 to 12.0. This is attributed to the decreased $\Delta c_{Na^+}/c_{Na^+,0}$
258 as the decrease of anode Na^+ concentration inside this concentration range. The normalized
259 concentration of NH_4^+ is relatively stable (60.2% - 61.3%) when the anode Na^+ concentration
260 varies from 1 mmol·L^{-1} to 8 mmol·L^{-1}, leading to a stable $\Delta c_{NH_4^+}/c_{NH_4^+,0}$ when calculating
261 selectivity. Interestingly, when the anode Na^+ concentration is higher than 8 mmol·L^{-1}, increasing
262 the anode Na^+ concentration also increases the selectivity. For example, when the anode Na^+
263 concentration is 120 mmol·L^{-1}, the selectivity is 6.4, which is 51.6% higher than the selectivity at
264 8 mmol·L^{-1}. The increase in selectivity can be explained by the increasing $c_{Na^+,0}$ and relatively
265 stable numbers of both $\Delta c_{NH_4^+}/c_{NH_4^+,0}$ and Δc_{Na^+}.

266 As anode Na^+ concentration increases, we observe a decline in both the ammonia recovery
267 amount Q_{NH_3} and ammonia recovery efficiency η_{NH_3}, which is unsurprising as the amount of
268 transported Na^+ increases. Notably, the decrease in both parameters becomes more significant
269 when the anode Na^+ concentration exceeds 8 mmol·L^{-1}. For example, when the anode Na^+
270 concentration is 2 mmol·L-1, Q_{NH_3} and η_{NH_3} are 2.74 mmol and 24.33 %, respectively. Q_{NH_3} is
271 reduced by 1.0% and 12.2% when the anode Na^+ concentrations are 10 mmol·L-1 and 200

mmol·L-1, respectively. Same trend is observed for η_{NH_3}. This phenomenon also confirms that ion competition significantly affects the system performance when the anode Na^+ concentration is higher than 8 mmol·L^{-1}.

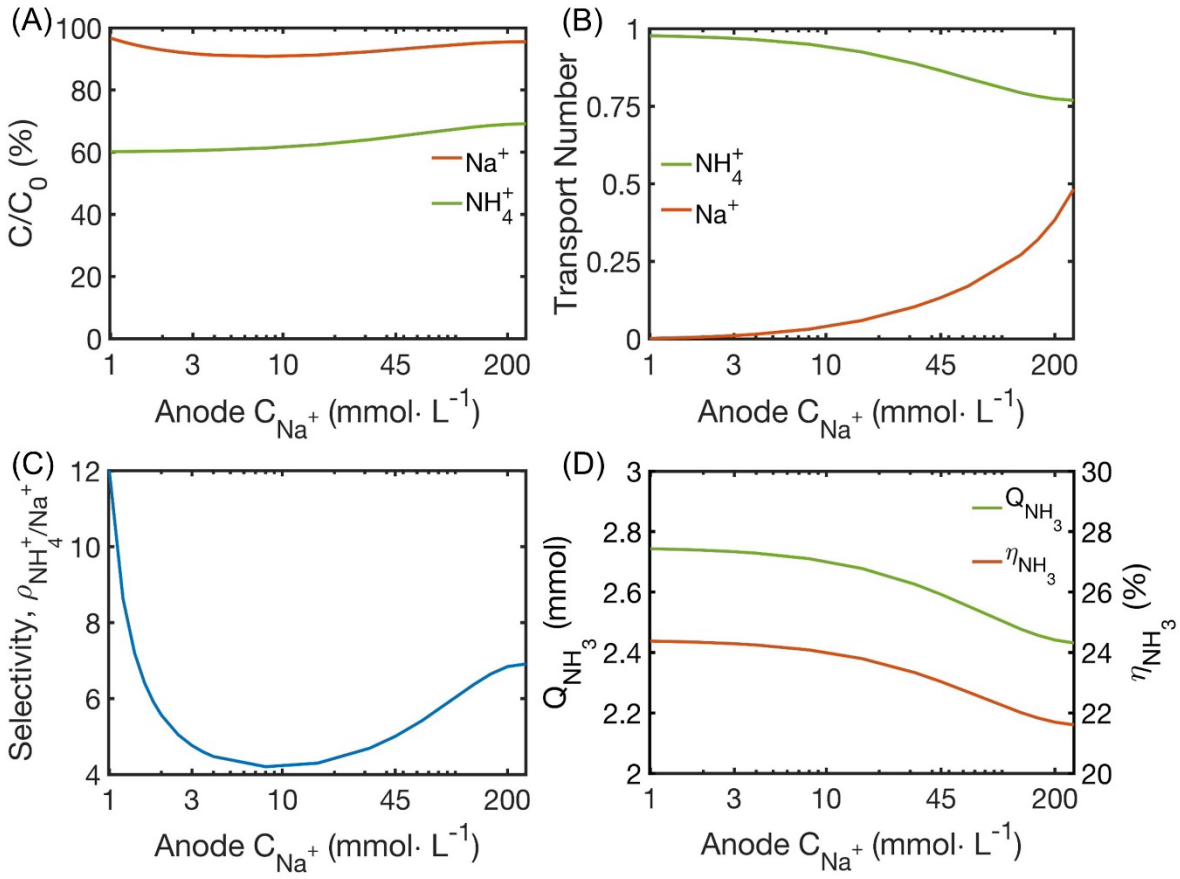

Figure 3. Selective ammonia recovery for varying initial anode Na^+ concentration. The initial concentrations of NH_4^+ in the anode is 55 mmol·L^{-1}. (A) Normalized final concentrations of Na^+ (orange line) and NH_4^+ (green line) ions in the anode. C is the ion concentration at the end of each cycle, while C_0 is the initial ion concentration in the anode. (B) Transport number of Na^+ (orange

line) and NH_4^+ (green line) ions. (C) Selectivity of NH_4^+/ Na^+ across the membrane-solution interface. (D) Ammonia recovery amount and efficiency. Green line is recovery amount and orange line is recovery efficiency.

3.3 Effect of Na^+ fraction in the anode

In addition, we vary the initial Na^+ concentration fraction in anolyte from 10% to 90% while maintaining the total cation ($Na^+ + NH_4^+$) concentration at 100 mmol·L^{-1}. Compared to varying the initial Na^+ concentrations from 1 mmol·L^{-1} to 200 mmol·L^{-1} in anolyte, varying the initial Na^+ concentration fraction in anolyte leads to a more significant decrease for the normalized concentration of NH_4^+ in anolyte as the increasing Na^+ concentrations (Fig. 4A). For example, varying the initial Na^+ concentration fraction in anolyte from 10% to 90% results in the normalized NH_4^+ concentration changing from 75.7% to 3.97%, which is a more notable depletion compared to that of changing the initial Na^+ concentrations in anolyte from 1 to 200 mmol·L^{-1} (normalized NH_4^+ concentration from 60.2% to 69.1%). However, the normalized Na^+ concentration is relatively stable. It changes from 95.1% to 85.7% when the Na^+ concentration fraction changes from 10% to 90%.

The transport number profiles in Fig. 4B reveal more explicit NH_4^+ and Na^+ ion transfer behaviors. At the initial Na^+ fraction of 10%, the transport numbers of NH_4^+ and Na^+ ions are 0.979

297 and 0.021, respectively. As the initial Na^+ fraction increases, there is a continuous decrease in the
298 transport number of NH_4^+ while the transport number of Na^+ correspondingly increases. The NH_4^+
299 transport number is always higher than the transport number of Na^+ ion when the initial Na^+
300 fraction ranges from 10% to 88.5%. For example, at the initial Na^+ fraction of 50%, where both
301 NH_4^+ and Na^+ concentrations are 50 mmol·L^{-1}, the transport numbers of NH_4^+ and Na^+ ion are 0.843
302 and 0.157, respectively. Such difference indicates the NH_4^+ ion transport is more preferred than the
303 Na^+ ion, which is consistent with the conclusion from section 3.2.

304 As shown in Fig. 4C, the NH_4^+/ Na^+ selectivity value consistently exceeds 4.68 across the range
305 of initial Na^+ fraction changes, indicating that the NH_4^+ ion is easier to be transferred to the cathode
306 compartment compared to the Na^+ ion. The lowest and highest selectivity is 4.68 and 7.02,
307 respectively, when the initial Na^+ fraction is 20% and 86%. Within this Na^+ fraction range, we
308 observe a continuous increase in the selectivity. Such a trend is attributed to the steadily decreasing
309 NH_4^+ concentration in anolyte, which increases $\Delta c_{NH_4^+}/c_{NH_4^+,0}$ and keeps $\Delta c_{Na^+}/c_{Na^+,0}$ at a
310 relatively stable value. However, we note that at the initial Na^+ fraction from 10% to 20% and from
311 86% to 90%, the NH_4^+/ Na^+ selectivity shows the reverse trend, potentially due to the extremely
312 small value of $c_{NH_4^+,0}$ and $c_{Na^+,0}$, respectively.

313 As demonstrated in Fig. 4D, the increase of initial Na^+ fraction leads to a decrease in the initial
314 NH_4^+ concentration and thereby a decreasing ammonia recovery amount (Q_{NH_3}). For example,

315 Q_{NH_3} changes from 2.74 mmol to 1.75 mmol as the initial Na^+ fraction varies from 10% to 90%.

316 However, the ammonia recovery efficiency (η_{NH_3}) exhibits an opposite trend: it continuously

317 increases from 15.0% to 77.6% as the initial Na^+ fraction varies from 10% to 90%. This trend is

318 attributed to the decrease of the initial ammonia concentration $c_{NH_4^+,0}$.

319

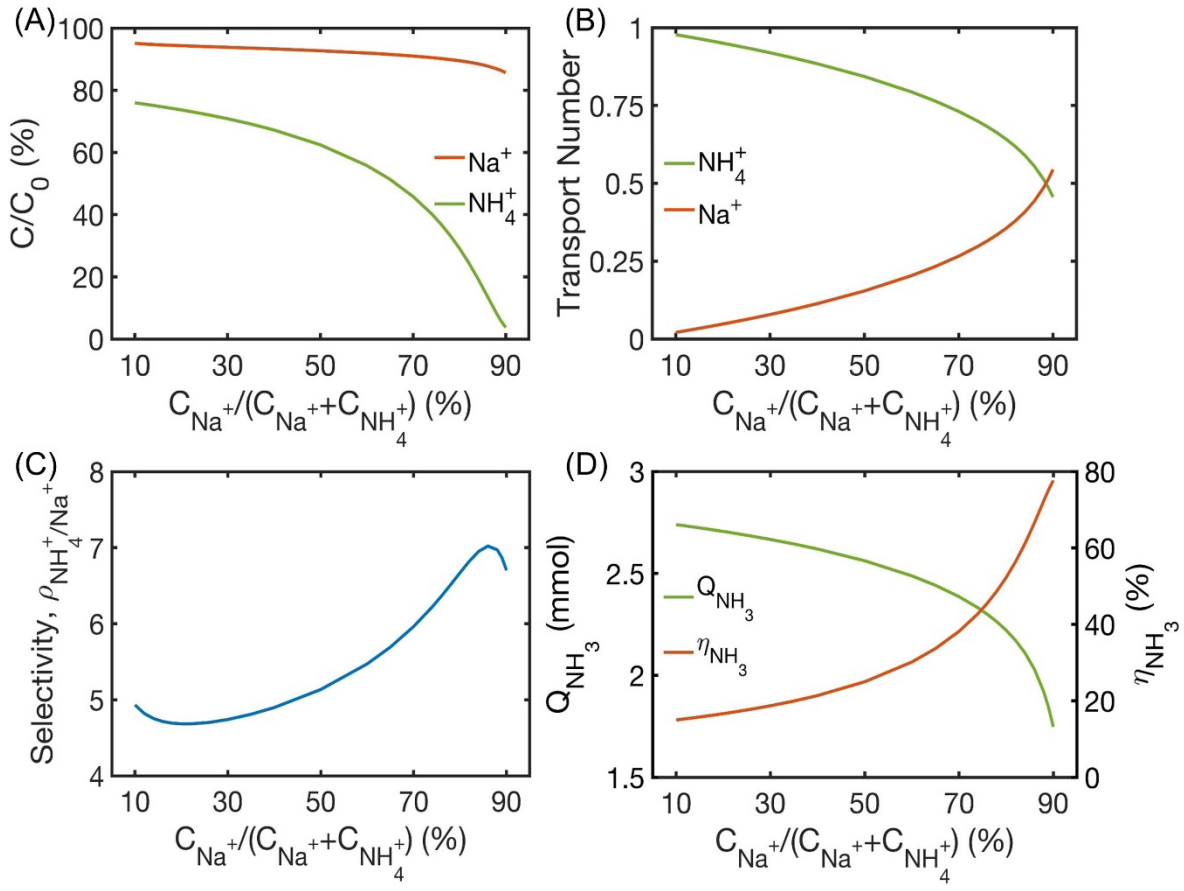

320

Figure 4. Selective ammonia recovery for varying anode Na^+ and NH_4^+ fractions in the anode. The total concentrations of NH_4^+ and Na^+ in the anode is 100 $mmol \cdot L^{-1}$. All other initial ion concentrations remain unchanged. The current density in every single simulation linearly decreases from 2 $A \cdot m^{-2}$ to 0.5 $A \cdot m^{-2}$. (A) Normalized final concentrations of Na^+ (orange line) and NH_4^+ (green line) ions in the anode. C is the ion concentration at the end of each cycle, while C_0 is the initial ion concentration in the anode. (B) Transport number of Na^+ (orange line) and NH_4^+ (green line) ions. (C) Selectivity of NH_4^+/ Na^+ across the membrane-solution interface. (D) Ammonia recovery amount and efficiency. The green line is the recovery amount and the orange line is recovery efficiency.

3.4 Na^+ in the cathode enhances NH_4^+ transport

In the previous sections, we explore the effects of initial Na^+ concentration and fraction on the transport of both NH_4^+ and Na^+ ions. While the transport of NH_4^+ dominantly governs ion transport across the membrane, the transport of Na^+ from anolyte to catholyte cannot be eliminated. To minimize Na^+ transport, we utilize Donnan Dialysis and add additional Na^+ ions in the cathode solution. Donnan Dialysis is an ion exchange phenomenon driven by the difference in ion concentrations on both sides of the ion exchange membrane (Davis, 2000a; Sata, 2007). Although

Donnan Dialysis has been applied for metal recovery or ammonia recovery from wastewater, usually it is not integrated into an electrochemical process (Agarwal et al., 2016; Rodrigues et al., 2020). Therefore, we increase the initial Na^+ concentration at catholyte from 0.1 mmol· L^{-1} to 30 mmol· L^{-1}, while maintaining all other initial cation concentrations unchanged.

The normalized concentration of NH_4^+ and Na^+ shows opposite trends as a function of the initial cathode Na^+ concentration (Fig. 5A). As the initial cathode Na^+ concentration increases from 0.1 mmol· L^{-1} to 30 mmol· L^{-1}, the normalized NH_4^+ concentration decreases from 64.9% to 46.5% whereas the normalized Na^+ concentration increases from 93.0% to 115.7%. This value exceeds 100% and indicates that Na^+ ions are transported from the cathode compartment to the anode compartment. Furthermore, the normalized concentration of NH_4^+ remains consistently smaller than that of Na^+ regardless of the initial cathode Na^+ concentration, indicating that a larger portion of Na^+ ions remain in the anode compartment compared to NH_4^+ ions.

As depicted in Fig. 5B, the transport number of NH_4^+ exceeds that of Na^+ regardless of initial cathode Na^+ concentration, indicating that NH_4^+ transport dominates the charge transfer. The addition of Na^+ ions in the cathode compartment facilitates NH_4^+ transport since the transport number of NH_4^+ increases from 0.863 to 1.285 as the initial cathode Na^+ concentration increases from 0.1 mmol· L^{-1} to 30 mmol· L^{-1}. The increased NH_4^+ transport number highlights the importance of Na^+ ions in the cathode compartment. When the initial cathode Na^+ concentration

356 is small and close to 0 mmol· L^{-1}, its impact on both NH_4^+ and Na^+ ion transport is minimal.
357 Increasing the initial cathode Na^+ concentration from 0.1 mmol· L^{-1} to 1 mmol· L^{-1} only leads to
358 an increase of 2.3% (from 0.863 to 0.884) for the transport number of NH_4^+. As a comparison, the
359 transport number of Na^+ drops 15.1% (from 0.133 to 0.113). In this situation, the Na^+ ion still
360 transport from the anode compartment to the cathode compartment. The selectivity of NH_4^+/ Na^+
361 for this cathode Na^+ concentration range is quite stable, as shown in Fig. 5C. When the initial
362 cathode Na^+ concentration increases from 0.1 mmol· L^{-1} to 1 mmol· L^{-1}, the selectivity of NH_4^+/
363 Na^+ increases by 20.7% (from 5.01 to 6.05) due to a consistent decrease in Δc_{Na^+} and an increase
364 in $\Delta c_{NH_4^+}$.

365 When the initial cathode Na^+ concentration reaches a critical value, 6.8 mmol· L^{-1}, the transport
366 number of NH_4^+ equals to 1 while the transport number of Na^+ is 0. In this scenario, there is no
367 overall Na^+ transport and all the electrons transfer through external circuit is exclusively used for
368 the transport of NH_4^+. Hence, the selectivity of NH_4^+/ Na^+ does not possess a reasonable value
369 since Δc_{Na^+} is zero. As the initial cathode Na^+ concentration exceeds 6.8 mmol· L^{-1}, the transport
370 number of NH_4^+ is greater than 1 while the transport number of Na^+ has a negative value,
371 confirming that a reverse Na^+ flux from catholyte to anolyte exists. As a result, the amount of NH_4^+
372 transport surpasses the charge transfer and the selectivity of NH_4^+/Na^+ is negative due to a negative

373 value of Δc_{Na^+}. Based on the results, we conclude that Donnan Dialysis could enhance the
374 transport of NH_4^+ ions in electrochemical systems.

375 We note that a high concentration of Na^+ ions in the cathode compartment is beneficial to
376 ammonia recovery in electrochemical cells. Both the ammonia recovery amount Q_{NH_3} and
377 ammonia recovery efficiency η_{NH_3} increase with the increasing initial cathode Na^+ concentration
378 due to the elevating NH_4^+ transport. As the initial cathode Na^+ concentration rises from 0.1 mmol·
379 L^{-1} to 30 mmol· L^{-1}, the Q_{NH_3} increases from 2.59 mmol to 3.05 mmol while the η_{NH_3} increases
380 from 23.1% to 27.2%.

381

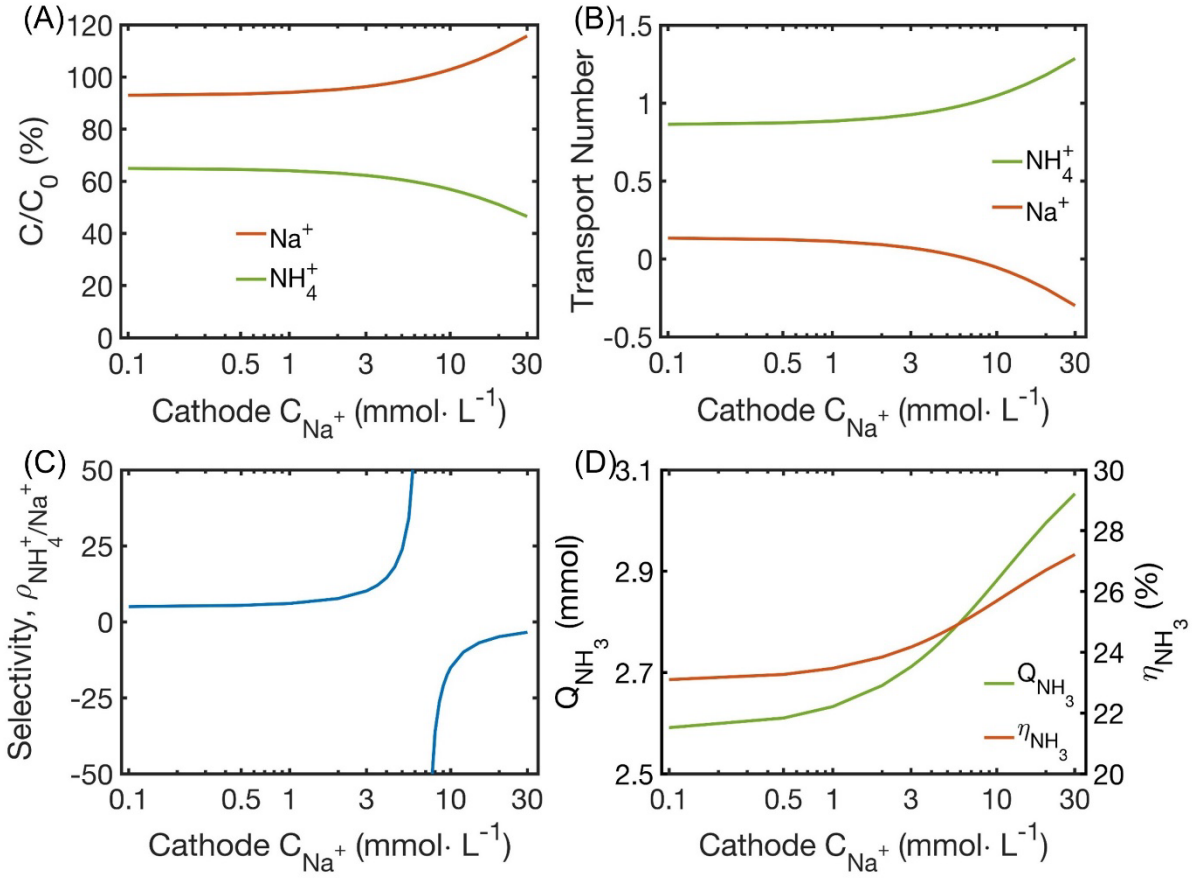

382

383 **Figure 5.** Selective ammonia recovery for varying initial cathode Na^+ concentration. The initial
384 cathode Na^+ concentration varies from 0.1 mmol· L^{-1} to 30 mmol· L^{-1}. All other initial ion
385 concentrations remain unchanged. The current density in every single simulation linearly
386 decreases from 2 A/m^2 to 0.5 A/m^2. (A) Normalized final concentrations of Na^+ (orange line) and
387 NH_4^+ (green line) ions in the anode. C is the ion concentration at the end of each cycle, while C_0
388 is the initial ion concentration in the anode. (B) Transport number of Na^+ (orange line) and NH_4^+
389 (green line) ions. (C) Selectivity of NH_4^+/ Na^+ across the membrane-solution interface. (D)

390 Ammonia recovery amount and efficiency. Green line is recovery amount and orange line is
391 recovery efficiency.

392

393 *3.5 Discussion and Perspective*

394 Membrane electrochemical systems serve as a versatile platform for various applications,
395 including wastewater treatment, resource recovery, power generation, and sensing platforms for
396 contamination detection. In this study, we simulated the ion concentration profiles and variations,
397 transport numbers, ammonia recovery rates, and recovery efficiencies to predict the NH_4^+ transport
398 with the presence of other ions in MES. Specifically, we focused on the NH_4^+ transport with the
399 presence of Na^+ ions to gain insights into ammonia recovery from wastewater. We found that the
400 imbalanced Na^+ ion concentration across the membrane is associated with the Donnan equilibrium
401 to facilitate the Na^+ transport, which is consequently impacted by the Na^+ ion concentration
402 distribution in the MES. According to the simulation results, Na^+ ions in anolyte act as competing
403 cations since they are prevalent in wastewater in a stable form. While in catholyte, Na^+ ions
404 facilitate the NH_4^+ transport and recovery.

405 The mathematical model was constructed based on a bioanode MES reactor in batch mode. As
406 the organic matters are consumed by the microorganisms at the bioanode, the current generation
407 decreases, affecting the ion transport, pH gradients across cation exchange membrane, and Donnan

equilibrium. The simulation captured those changes within a batch cycle, showing how the parameters affect one another. We note that a continuous mode would be preferred when scaling up the MES for real-world applications. Additionally, scaling up the MES necessitates additional investigation due to the complexities of ion movement in the bulk anolyte or catholyte, instead of assuming well-mixed in the small volume of this lab-scale MES reactor. To investigate the ion movement in scaled up system, a series of experiments need to be conducted to explore the effect of membrane area, anolyte compartment thickness and volume on the ion movement. However, this lab-scale simulation can still provide insight into the selective ion transport toward ammonia recovery.

In this study, microorganisms were inoculated in the MES anode to degrade organic matters while oxygen was used as the electron acceptor. This setup allowed MES to function through spontaneous bioelectrochemical reactions without external energy input. Therefore, energy efficiency, which is typically analyzed in electrochemical cells, was not calculated and discussed here since the primary aim was to improve the ammonium transport and recovery efficiency in the self-sustained MES. We believe that using MES to achieve ammonia recovery is a sustainable approach since this spontaneous process separates ammonium ions from wastewater and collects them as valuable fertilizer products, mitigating the contamination to the environment and preserving the energy from the Haber-Bosch process.

4. CONCLUSION

In this study, we utilize a mathematical model to reveal the selective NH_4^+ transport across a cation exchange membrane in the presence of Na^+, an inert cation that commonly co-exists with ammonium in wastewater. Specifically, we analyzed the concentration profile of both NH_4^+ and Na^+ in the bulk solution and the membrane. Through comprehensive evaluation of Na^+ concentrations in the system, we derived several performance matrices of this membrane electrochemical system, such as normalized concentration variation with time, transport number, selectivity, and ammonia recovery amount and efficiency. The presence of Na^+ as an inert cation in the anode compartment impacts the ammonia recovery since the Na^+ transport competes with the NH_4^+ transport. However, in most cases, the NH_4^+ transport dominates the total cation transport unless the NH_4^+ concentration fraction in the anode compartment is extremely low (~11.5%). More significantly, the presence of Na^+ in the cathode compartment facilitates the ammonia transport because of Donnan Dialysis. The analyses offer important insights into the practical application of ammonia recovery via membrane electrochemical system by incorporating the addition of inert cations to enhance ammonia recovery selectivity and efficiency.

AUTHOR AGREEMENT

All authors are aware of and accept responsibility for the manuscript. This manuscript has not been previously published, in whole or in part, and it is not under consideration by any other journal.

AUTHOR CONTRIBUTION

Kai Yang: Investigation, Methodology, Formal analysis, Validation, Visualization, Writing - original draft. Mohan Qin: Conceptualization, Methodology, Writing - review & editing, Funding acquisition.

AUTHOR CONTRIBUTION

The authors would like to thank the support from National Science Foundation CBET 2219089. In addition, the authors would like to thank the startup fund from the Department of Civil and Environmental Engineering, College of Engineering, the Office of the Vice-Chancellor for Research and Graduate Education (OVCRGE) at the University of Wisconsin-Madison, and the Wisconsin Alumni Research Foundation (WARF) for the support of this study.

REFERENCES

Agarwal, C., Cattrall, R.W. and Kolev, S.D. 2016. Donnan dialysis based separation of gold(III) from electronic waste solutions using an anion exchange pore-filled membrane. J. Membr. Sci. 514, 210-216.

Burns, M. and Qin, M. 2023. Ammonia recovery from organic nitrogen in synthetic dairy manure with a microbial fuel cell. Chemosphere 325, 138388.

Capdevila-Cortada, M. 2019. Electrifying the Haber–Bosch. Nat. Catal. 2(12), 1055-1055.

Chen, C., Dong, T., Han, M.Y., Yao, J.M. and Han, L. 2020. Ammonium recovery from wastewater by Donnan Dialysis: A feasibility study. J. Clean. Prod. 265.

Chen, C., Han, M., Yao, J., Zhi, Y., Liu, Y., Zhang, C. and Han, L. 2021. Donnan Dialysis-Osmotic Distillation (DD-OD) Hybrid Process for Selective Ammonium Recovery Driven by Waste Alkali. Environ Sci Technol 55(10), 7015-7024.

Chen, J.G., Crooks, R.M., Seefeldt, L.C., Bren, K.L., Bullock, R.M., Darensbourg, M.Y., Holland, P.L., Hoffman, B., Janik, M.J., Jones, A.K., Kanatzidis, M.G., King, P., Lancaster, K.M., Lymar, S.V., Pfromm, P., Schneider, W.F. and Schrock, R.R. 2018. Beyond fossil fuel-driven nitrogen transformations. Science 360(6391).

Cord-Ruwisch, R., Law, Y. and Cheng, K.Y. 2011. Ammonium as a sustainable proton shuttle in bioelectrochemical systems. Bioresour. Technol. 102(20), 9691-9696.

Davis, T. 2000a. Donnan dialysis. Encyclopedia of separation science 4, 1701-1707.

Davis, T. 2000b. Donnan dialysis. Membrane Separations 2, 1701-1707.

Dawson, C.J. and Hilton, J. 2011. Fertiliser availability in a resource-limited world: Production and recycling of nitrogen and phosphorus. Food Policy 36, S14-S22.

Epsztein, R., Shaulsky, E., Qin, M. and Elimelech, M. 2019. Activation behavior for ion permeation in ion-exchange membranes: Role of ion dehydration in selective transport. J. Membr. Sci. 580, 316-326.

Ertl, G. 1990. Elementary Steps in Heterogeneous Catalysis. Angew. Chem., Int. Ed. Engl. 29(11), 1219-1227.

Fang, K., Gong, H., He, W.Y., Peng, F., He, C.H. and Wang, K.J. 2018. Recovering ammonia from municipal wastewater by flow-electrode capacitive deionization. J. Chem. Eng. 348, 301-309.

Galloway, J.N., Dentener, F.J., Capone, D.G., Boyer, E.W., Howarth, R.W., Seitzinger, S.P., Asner, G.P., Cleveland, C.C., Green, P. and Holland, E.A. 2004a. Nitrogen cycles: past, present, and future. Biogeochemistry 70(2), 153-226.

Galloway, J.N., Dentener, F.J., Capone, D.G., Boyer, E.W., Howarth, R.W., Seitzinger, S.P., Asner, G.P., Cleveland, C.C., Green, P.A., Holland, E.A., Karl, D.M., Michaels, A.F.,

Porter, J.H., Townsend, A.R. and Vöosmarty, C.J. 2004b. Nitrogen Cycles: Past, Present, and Future. Biogeochemistry 70(2), 153-226.

He, C., Ma, J., Zhang, C., Song, J. and Waite, T.D. 2018. Short-Circuited Closed-Cycle Operation of Flow-Electrode CDI for Brackish Water Softening. Environ Sci Technol 52(16), 9350-9360.

Jacobsen, C.J.H., Dahl, S., Clausen, B.S., Bahn, S., Logadottir, A. and Nørskov, J.K. 2001. Catalyst Design by Interpolation in the Periodic Table: Bimetallic Ammonia Synthesis Catalysts. J. Am. Chem. Soc. 123(34), 8404-8405.

Kim, J.R., Zuo, Y., Regan, J.M. and Logan, B.E. 2008. Analysis of ammonia loss mechanisms in microbial fuel cells treating animal wastewater. Biotechnol. Bioeng. 99(5), 1120-1127.

Kuntke, P., Rodriguez Arredondo, M., Widyakristi, L., Ter Heijne, A., Sleutels, T.H., Hamelers, H.V. and Buisman, C.J. 2017. Hydrogen Gas Recycling for Energy Efficient Ammonia Recovery in Electrochemical Systems. Environ Sci Technol 51(5), 3110-3116.

Kuntke, P., Smiech, K.M., Bruning, H., Zeeman, G., Saakes, M., Sleutels, T.H., Hamelers, H.V. and Buisman, C.J. 2012. Ammonium recovery and energy production from urine by a microbial fuel cell. Water Res. 46(8), 2627-2636.

Ledezma, P., Kuntke, P., Buisman, C.J.N., Keller, J. and Freguia, S. 2015. Source-separated urine opens golden opportunities for microbial electrochemical technologies. Trends Biotechnol. 33(4), 214-220.

Lee, G., Kim, K., Chung, J. and Han, J.I. 2020. Electrochemical ammonia accumulation and recovery from ammonia-rich livestock wastewater. Chemosphere, 128631.

Liu, M.J., Neo, B.S. and Tarpeh, W.A. 2020. Building an operational framework for selective nitrogen recovery via electrochemical stripping. Water Res. 169, 115226.

Liu, Y., Qin, M., Luo, S., He, Z. and Qiao, R. 2016. Understanding Ammonium Transport in Bioelectrochemical Systems towards its Recovery. Sci. Rep. 6, 22547.

Luo, T., Abdu, S. and Wessling, M. 2018. Selectivity of ion exchange membranes: A review. J. Membr. Sci. 555, 429-454.

Park, C., Muller, C.D., Abu-Orf, M.M. and Novak, J.T. 2006. The effect of wastewater cations on activated sludge characteristics: effects of aluminum and iron in floc. Water Environ Res 78(1), 31-40.

Qin, M. and He, Z. 2014. Self-Supplied Ammonium Bicarbonate Draw Solute for Achieving Wastewater Treatment and Recovery in a Microbial Electrolysis Cell-Forward Osmosis-Coupled System. Environ. Sci. Technol. Lett. 1(10), 437-441.

Qin, M., Molitor, H., Brazil, B., Novak, J.T. and He, Z. 2016. Recovery of nitrogen and water from landfill leachate by a microbial electrolysis cell-forward osmosis system. Bioresour. Technol. 200, 485-492.

526 Rodrigues, M., Lund, R.J., ter Heijne, A., Sleutels, T., Buisman, C.J.N. and Kuntke, P. 2022a.
527 Application of ammonium fertilizers recovered by an Electrochemical System. Resour.
528 Conserv. Recycl. 181, 106225.
529 Rodrigues, M., Sleutels, T., Kuntke, P., Buisman, C.J.N. and Hamelers, H.V.M. 2022b. Effects
530 of Current on the Membrane and Boundary Layer Selectivity in Electrochemical Systems
531 Designed for Nutrient Recovery. ACS Sustain. Chem. Eng. 10(29), 9411-9418.
532 Rodrigues, M., Sleutels, T., Kuntke, P., Hoekstra, D., ter Heijne, A., Buisman, C.J.N. and
533 Hamelers, H.V.M. 2020. Exploiting Donnan Dialysis to enhance ammonia recovery in
534 an electrochemical system. J. Chem. Eng. 395.
535 Rodríguez Arredondo, M., Kuntke, P., Jeremiasse, A.W., Sleutels, T.H.J.A., Buisman, C.J.N. and
536 ter Heijne, A. 2015. Bioelectrochemical systems for nitrogen removal and recovery from
537 wastewater. Environ. Sci.: Water Res. Technol. 1(1), 22-33.
538 Sata, T. (2007) Ion exchange membranes: preparation, characterization, modification and
539 application, Royal Society of Chemistry.
540 Strathmann, H. 2010. Electrodialysis, a mature technology with a multitude of new
541 applications. Desalination 264(3), 268-288.
542 Tarpeh, W.A., Barazesh, J.M., Cath, T.Y. and Nelson, K.L. 2018. Electrochemical Stripping to
543 Recover Nitrogen from Source-Separated Urine. Environ. Sci. Technol. 52(3), 1453-
544 1460.
545 Van der Hoek, J., Duijff, R. and Reinstra, O. 2018. Nitrogen Recovery from Wastewater:
546 Possibilities, Competition with Other Resources, and Adaptation Pathways. Sustainability
547 10(12).
548 Yang, K., Du, H.A. and Qin, M.H. 2023. Solar enhanced membrane distillation for ammonia
549 recovery. J. Membr. Sci. Lett. 3(1), 100043.
550 Yang, K. and Qin, M. 2021. The Application of Cation Exchange Membranes in
551 Electrochemical Systems for Ammonia Recovery from Wastewater. Membranes 11(7),
552 494.
553 Ye, Z.L., Ghyselbrecht, K., Monballiu, A., Pinoy, L. and Meesschaert, B. 2019. Fractionating
554 various nutrient ions for resource recovery from swine wastewater using simultaneous
555 anionic and cationic selective-electrodialysis. Water Res. 160, 424-434.
556 Zamora, P., Georgieva, T., Ter Heijne, A., Sleutels, T.H.J.A., Jeremiasse, A.W., Saakes, M.,
557 Buisman, C.J.N. and Kuntke, P. 2017. Ammonia recovery from urine in a scaled-up
558 Microbial Electrolysis Cell. J. Power Sources 356, 491-499.
559 Zhang, Y. and Angelidaki, I. 2015a. Recovery of ammonia and sulfate from waste streams and
560 bioenergy production via bipolar bioelectrodialysis. Water Res. 85, 177-184.

Zhang, Y. and Angelidaki, I. 2015b. Submersible microbial desalination cell for simultaneous ammonia recovery and electricity production from anaerobic reactors containing high levels of ammonia. Bioresour. Technol. 177, 233-239.
Zou, S., Qin, M., Moreau, Y. and He, Z. 2017. Nutrient-energy-water recovery from synthetic sidestream centrate using a microbial electrolysis cell - forward osmosis hybrid system. J. Clean. Prod. 154, 16-25.